

Generation of droplet group based on an external electromagnetic valve in a microfluidic chip

Dong Wang(王东), Xiaonan Li(李啸楠), Jiayi Zhou(周佳怡), Liyu Liu(刘雳宇), and Guo Chen(陈果)
Citation: Chin. Phys. B, 2025, 34 (**12**): 124702. DOI: 10.1088/1674-1056/ade063
http://cpb.iphy.ac.cn; http://iopscience.iop.org/cpb

What follows is a list of articles you may be interested in

Experimental study on characteristics of isopropanol ejection driven by electrohydrodynamics

Xi-Hao Zhang(张玺皓), Wen-Hua Wang (王文华), Cheng-Nan He(何承南), Yi-Chi Yao(姚奕弛), Bo-Yu Wang (王博宇), Xue-Hong Li(李学红), Zhi-Jian Wang(王智健), Chen Qiu(邱晨), Hai-Yi Sun(孙海轶), Yu-Xin Leng(冷雨欣), and Gang Xin(新刚)
Chin. Phys. B, 2025, 34 (**11**): 114701. DOI: 10.1088/1674-1056/addbcc

Computational and experimental investigations of a microfluidic mixer for efficient iodine extraction using carbon tetrachloride enhanced with gas bubbles

Siddique Muhammad Kashif, Sun Lin(孙林), and Li Songjing(李松晶)
Chin. Phys. B, 2023, 32 (**11**): 114702. DOI: 10.1088/1674-1056/acf03f

Nanobubbles produced by hydraulic air compression technique

Xiaodong Yang(杨晓东), Qingfeng Yang(杨庆峰), Limin Zhou(周利民),Lijuan Zhang(张立娟), and Jun Hu(胡钧)
Chin. Phys. B, 2022, 31 (**5**): 054702. DOI: 10.1088/1674-1056/ac464c

Crown evolution kinematics of a camellia oil droplet impacting on a liquid layer

Zhongyu Shi(石中玉), Guanqing Wang(王关晴), Xiangxiang Chen(陈翔翔), Lu Wang(王路), Ning Ding(丁宁), and Jiangrong Xu(徐江荣)
Chin. Phys. B, 2022, 31 (**5**): 054701. DOI: 10.1088/1674-1056/ac46c1

Droplets breakup via a splitting microchannel

Wei Gao(高崴), Cheng Yu(于程), Feng Yao(姚峰)
Chin. Phys. B, 2020, 29 (**5**): 054702. DOI: 10.1088/1674-1056/ab7b4b

---

Generation of droplet group based on an external electromagnetic valve in a microfluidic chip

Dong Wang(王东), Xiaonan Li(李啸楠), Jiayi Zhou(周佳怡),
Liyu Liu(刘雳宇)†, and Guo Chen(陈果)‡

Chongqing Key Laboratory of Interface Physics in Energy Conversion, School of Physics and Center of Quantum Materials and Devices, Chongqing University, Chongqing 401331, *China*

(Received 21 February 2025; revised manuscript received 22 May 2025; accepted manuscript online 4 June 2025)

Previous studies on droplet generation in microfluidics mainly focus on the monodisperse droplet, but limited attention has paid to the generation of droplet groups composed of multiple droplets with different volumes or components. In this study, a programmable electromagnetic valve is externally connected with the microfluidic chip featuring a conventional flow-focused structure. Different from the previous situation where only one droplet is generated by a single actuation of the electromagnetic valve, by precisely controlling the opening and closing of the valve, the continuous phase fluid exhibits periodic flow in the channel, and we realized the generation of a droplet group by a single actuation of the valve, and the number and volume of the droplets in each group can be regulated. Specifically, the number of large droplets in a droplet group is mainly determined by the opening time of the electromagnetic valve and the two-phase flow rate, and the number of small droplets is dominated by the valve closing time. The volume of individual droplets in a droplet group is largely dependent on the flow rate of the continuous phase. Our study extends the understanding of microfluidic droplet formation. It provides a feasible method for the efficient preparation of polydisperse droplets, which is important for microfluidic chip-based droplet control and has potential applications in industries related to microfluidic droplets.

Keywords: droplet group, electromagnetic valve, valve switching ratio, microfluidic chip

PACS: 47.55.db, 47.61.–k, 47.55.Ca, 47.55.D–

DOI: 10.1088/1674-1056/ade063 **CSTR:** 32038.14.CPB.ade063

1. Introduction

The applications of the microfluidic technology for the production of microdroplets with precisely controlled volume,[1–3] composition,[4,5] and quantity[6] have reached a high level of maturity. The microfluidic-based droplets have also been successfully used in various application scenarios including, but not limited to, enzyme assays,[7,8] drug screening,[9–11] nanocatalysts,[12,13] and biological reactions.[14,15] In microfluidics, the flow instability of the aqueous and oil phases when squeezing each other is usually utilized to form droplets, and the volume of the generated droplets depends on the flow rate of the two phases, and monodispersed droplets are generated at constant flow rate.[16,17] However, in some biological or chemical reactions based on microfluidics, there is a need for volume differentiation of droplets.[18] Therefore, regulating the volume of droplets in microfluidics has become an important concern, in which the introduction of valve devices to directly regulate the flow rate of microfluidic liquids is the most direct way to control the volume of droplets.[19] The principle is to generate a desired volume of droplets by controlling the opening and closing cycle of the valve. For example, by integrating a microvalve with a short response time into a microfluidic device, the formation and volume of a single droplet can be accurately and flexibly controlled through the opening and closing of the microvalve. However, the cost of microvalves is relatively high, and their dimensions often exceed those of the microchip structure, making integration challenging. To address these issues, several research teams have proposed relocating the valve outside the microfluidic chip to control over the flow of one or more liquids (continuous phase or dispersed phase) with high accuracy.[20] For relatively simple systems, this approach has proven effective, rendering external, off-the-shelf, and cost-effective valves a viable alternative to integrated microvalves. At present, whether it is a microvalve integrated in the chip or a commercial valve placed outside the chip, each opening and closing of the valve can only generate a specific size of the droplet.[21] There is a lack of research on how to reasonably adjust the opening and closing period of the valve so that it can produce multiple droplets with different volumes in one switching cycle.

In this study, we connect a commercial electromagnetic valve with a microfluidic device to investigate the formation rules of droplet groups through programmed control of the electromagnetic valve's opening and closing cycles. Specifically, the continuous phase fluid is passed through the commercial electromagnetic valve before being injected into the

†Corresponding author. E-mail: lyliu@cqu.edu.cn
‡Corresponding author. E-mail: wezer@cqu.edu.cn

© 2025 Chinese Physical Society and IOP Publishing Ltd. All rights, including for text and data mining, AI training, and similar technologies, are reserved.

microfluidic chip. The periodic actuation of the electromagnetic valve induces pulsed flow in the channel, leading to variations in droplet volume within the droplet groups generated in the flow-focused microchannel structure.[22] We find that each group of droplets consists of several droplets with two volumes, and the number of droplets of the two volumes is adjustable in proportion. This suggests that the periodic opening and closing of the electromagnetic valve can indeed produce droplet groups. Further studies show that the number of large droplets in each droplet group is determined by the opening time of the electromagnetic valve and the two-phase flow rate, the number of small droplets is determined by the closing time of the electromagnetic valve, and the volume of a single droplet in a droplet group is mainly dependent on the flow rate of the continuous phase. This study enriches the understanding of the formation of complex droplet systems using microfluidics and provides a new approach for the efficient preparation of polydisperse droplets.

2. Methods

2.1. Construction of the experimental setup

The schematic diagram of the whole experimental setup is shown in Fig. 1(a). The continuous phase was injected into the pipeline at Q_c flow rate by a syringe pump (LSP02-1B, Longer Precision Pump Company, China), flowed through an electromagnetic valve (VX213AAXNB, SMC, Japan) to form a pulsed flow, and then flowed into the continuous-phase channel of the microfluidic chip. The dispersed phase was injected directly into the dispersed phase channel of the chip via a syringe pump at the flow rate of Q_d. Both continuous and dispersed phase liquids were transported using 1-mm diameter PTFE capillary tubes during the experiments. The continuous phase of the pulsed flow, and the dispersed phase of the homogeneous flow formed droplets at the criss-cross of the chip, and the whole process of droplet formation was observed by a high-speed video camera (Phantom v7.3) attached to an inverted microscope (Olympus IX73) at a frame rate of 1000 s^{-1}.

2.2. Preparation of the continuous phase pulse flow

The formation of the continuous phase pulse flow was realized by using a laboratory-made digital controller to control the opening and closing of the electromagnetic valves. Each valve in the digital controller corresponds to a binary code Y. When this code is assigned a value of 1, the valve opens; when it is assigned a value of 0, the valve closes. Taking $T_{on} = 0.4$ s and $T_{off} = 0.3$ s as an example, so $Y_1 = 1$ and the execution time t_1 was set to 0.4 s and $Y_2 = 0$, and the execution time t_2 was set to 0.3 s. Since this was done continuously, the regulation was in cycle mode. The continuous phase changes from a constant flow rate to a pulsed flow when the syringe pump pushes a constant flow through the electromagnetic valve controlled by the digital controller with the setup completed data, as shown in Fig. 1(b).

2.3. Preparation of the chip

The chip was prepared by soft lithography. The photoresist (SU-8, 3025) with a thickness of about 100 μm is uniformly coated on a silicon wafer and heated to cure, the mask with the chip pattern is photolithographed on the silicon wafer, and the photoresist other than the chip pattern is rinsed off with the developer solution to complete the preparation of the chip mold. The chip material was a liquid mixture of polydimethylsiloxane (PDMS) and curing agent with a mass ratio of 10:1. The liquid was poured into the mold and cured at 80 °C for 4 h. Finally, it was tightly adhered to the slide.[23] After the above operations, the desired chip was made, as shown in Fig. 1(c). The chip is generally divided into two parts, the first half is a flow-focusing structure commonly used for the preparation of droplets, and the second half is a curved wrap-around channel designed for better observation of the droplets. The width of all channels in the chip is about 160 μm and the height is about 100 μm.

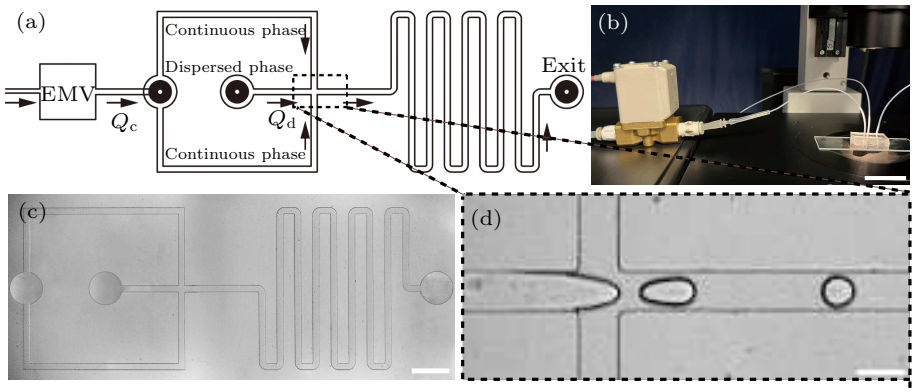


Fig. 1. (a) Cartoon diagram of the experimental setup showing the connection of electromagnetic valve (EMV) and microfluidic chip structure. (b) Physical photograph of the experimental setup (partial), showing how the valve is connected to the microfluidic chip through the continuous phase piping. The scale bar is 30 mm. (c) Image of the microfluidic chip. The scale bar is 1 mm. (d) Snapshot from fast photography showing the formation of the droplet in a flow-focused structure. The scale bar is 200 μm.

2.4. Preparation of microfluidic droplets

Droplets have to be produced by two immiscible liquids, in the experiment the continuous phase was a mixture of mineral oil (M195121 Aladdin) and the surfactant sorbitan oleate (Span 80) (0.5% w/w), and the dispersed phase was a mixture of deionized water and glycerol in a ratio of 1:1 by volume, and the surfactant was used to prevent the droplets from merging on contact. Figure 1(d) shows an example of droplets of different sizes generated at a flow-focusing type structure.

3. Results and discussion

3.1. Effect of electromagnetic valve opening time and closing time on the droplet group

First, the effect of the opening time of the electromagnetic valve on the droplet group was investigated. Figure 2(a) shows that under the conditions of valve closing time $T_{\text{off}} = 0.3$ s, continuous phase flow rate $Q_{\text{c}} = 3$ μL/min, and dispersed phase flow rate $Q_{\text{d}} = 0.5$ μL/min, groups of droplets are formed in the microfluidic channel by gradually increasing the valve opening time T_{on}, and the total generation time of each group of droplets is exactly equal to the duration of one cycle of valve opening and closing. To make the presentation of the droplet group clearer, we have marked the large droplets in red and the small ones in blue in one of the droplet groups under each set of conditions. It can be seen that with the valve opening time T_{on} increasing from 0.2 s to 1 s, the number of small droplets in each group is always maintained as 1, but the number of large droplets increases from 2 to 6, and correspondingly the total number of droplets in each droplet group increases from 3 to 7. This indicates that the opening time of the valve is positively correlated with the number of large droplets in the droplet group, but has little relationship with the number of small droplets.

The closing time of the electromagnetic valve also affects the formation of the droplet group. Figure 2(b) shows that under the conditions of valve opening time $T_{\text{on}} = 0.2$ s, continuous phase flow rate $Q_{\text{c}} = 3$ μL/min, and dispersed phase flow rate $Q_{\text{d}} = 0.5$ μL/min, the droplets in the microfluidic chip still appear in the form of groups as the valve closing time T_{off} is gradually increased from 0.45 s to 1 s. Moreover, the number of large droplets in each group is maintained at 2, and the number of small droplets increases from 2 to 6 in turn, and correspondingly the total number of droplets in each group increases from 4 to 8, which indicates that the closing time of the valve is positively correlated with the number of small droplets in the drop group, but has no effect on the number of large droplets.

Figure 2(c) plots the number details of the large and small droplets in each droplet group as the valve opening time and valve closing time change. We define the valve switching ratio as $\beta = T_{\text{on}}/T_{\text{off}}$. It can be seen more clearly that, on the one hand, when the valve opening time is unchanged, the number of large droplets (hollow circle) in each droplet group remains the same, and when the valve opening time is increased, the number of large droplets shows a linear increase. On the other hand, when the valve closing time is unchanged, the number of small droplets (solid circle) in each drop group remains the same, and when the valve closing time is increased, the number of small droplets shows a monotonic increase. These results are quite counterintuitive because increasing the valve opening time means that the continuous phase continues to be injected at a larger flow rate for a longer time, and the more strongly the dispersed phase is squeezed, the number of small droplets should increase, rather than the experimentally observed increase in the number of large droplets. Similarly, increasing the closing time of the valve should mean an increase in the number of large droplets, not small ones. We speculate that the reason for the discrepancy between the experimental observations and common sense is the sudden change in flow rate caused by the unwanted pressure pulses due to the periodic opening and closing of the electromagnetic valve.[24] Further, we use α to denote the ratio of the number of large droplets to small droplets in the droplet group, where $\alpha = N_{\text{large}}/N_{\text{small}}$. As shown in Figs. 2(d) and 2(e), the quantity ratio of large and small droplets in each droplet group is highly linearly correlated with the valve switching ratio. According to the linear fitting curves, it can be seen that their quantitative relationships are $\alpha = 1.5\beta + 0.9997$ and $\alpha^{-1} = 1.067\beta^{-1} - 0.523$ respectively, and the linear correlation coefficients of the fitted straight lines R^2 are 1 and 0.9947 respectively. The fitting coefficients all reached or approached 1, indicating that the valve switching ratio has a very strong regulatory effect of the droplet quantity ratio.

Figures 2(f)–2(g) show the effect of valve opening time T_{on} and valve closing time T_{off} on the volume of a single large droplet (hollow circle), a single small droplet (solid circle), and the volume of all droplets (solid triangles) in each group, respectively. The data shows that the change in the switching time of the electromagnetic valve alone does not significantly change the volume of each large or small droplet in the droplet group. However, the total volume of droplets in each drop group increases monotonically with the length of time the valve is opened or closed. Because either the increase in valve opening time (Fig. 2(f)) or the increase in valve closing time (Fig. 2(g)), it means that the opening and closing cycle time of the valve becomes longer, so the total volume of all droplets generated during that cycle naturally increases. The droplet volume measurements were taken from the first 4 droplet groups in the droplet image. The area of the droplet group image was measured using ImageJ, and the droplet volume is equal to the product of droplet area and chip height.

The standard deviation of the data was calculated using Origin to obtain the error bars in Figs. 2(f)–2(g). We have compared the total volume of each droplet group V_G measured experimentally with the predicted value (represented by solid lines) calculated according to the equation

$$V_G = Q_d \times (T_{on} + T_{off}) \tag{1}$$

and find the results are indeed highly consistent.

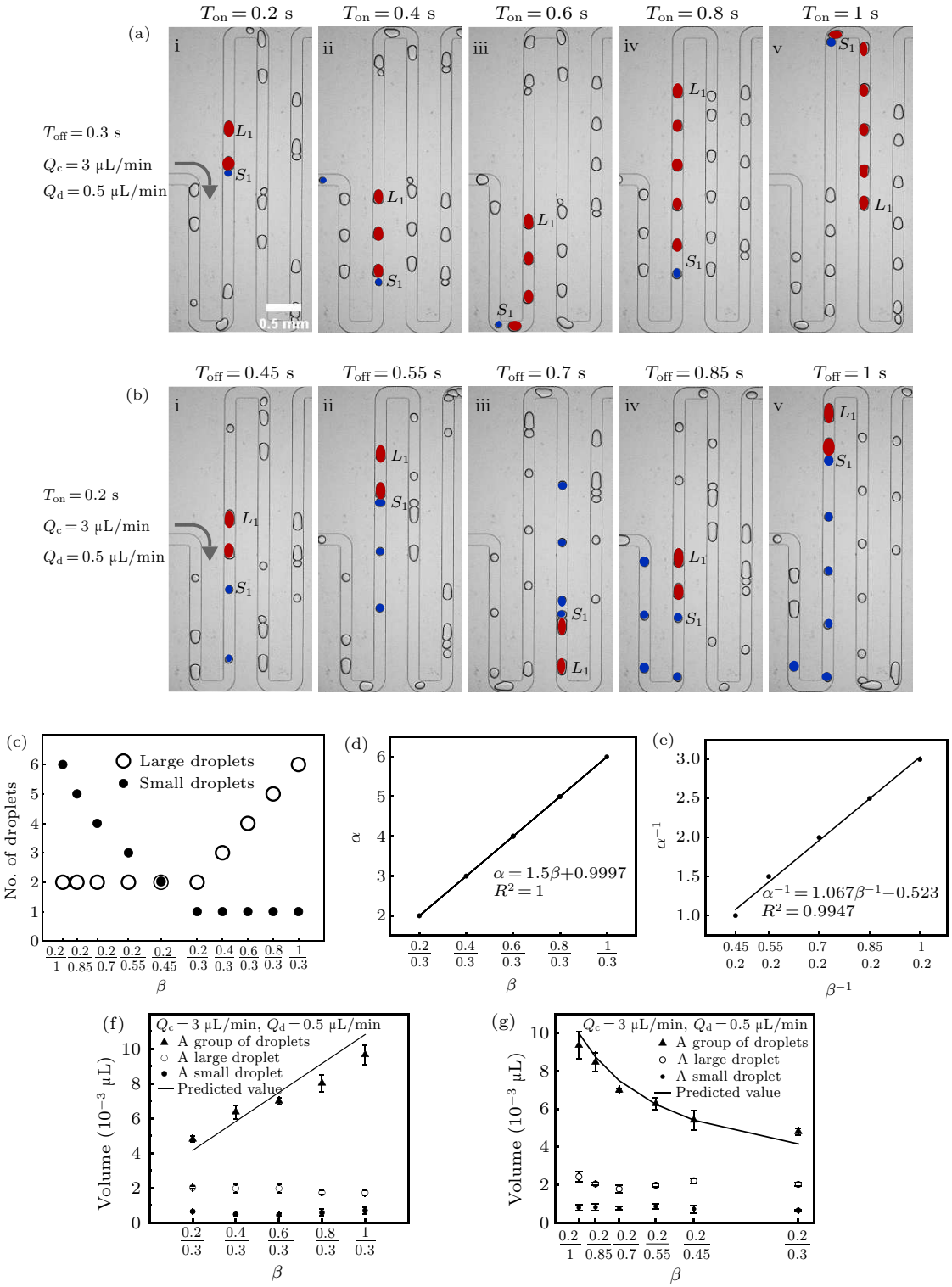


Fig. 2. (a) Representative images of droplet groups for five different valve opening times. The scale bar is 500 μm. (b) Representative images of droplet groups for five different valve closing times. (c) A plot of the number of droplets versus β. T_{on} is the valve opening time and T_{off} is the valve closing time. Hollow circles represent large droplets and solid circles represent small droplets. (d). Plot of droplet quantity ratio α versus valve switching ratio β when T_{on} is varied. (e) Plot of droplet number ratio α^{-1} versus valve switch ratio β^{-1} when T_{off} is varied. (f) and (g) Plots of droplet volume versus β. Solid triangle represents the volume of the droplet group, hollow circle represents the volume of a large droplet, and solid circle represents the volume of a small droplet. The solid line shows the predicted volume of droplet group.

Now, we can explain the linear relationship between the droplet quantity ratio α ($\alpha = N_{\text{large}}/N_{\text{small}}$) and the valve switching ratio β ($\beta = T_{\text{on}}/T_{\text{off}}$) given in Figs. 2(d) and 2(e).

Equation (1) can be rewritten as

$$V_{\text{G}} = Q_{\text{d}} \times T_{\text{off}} \times (\beta + 1) \tag{2}$$

or

$$V_{\text{G}} = Q_{\text{d}} \times T_{\text{on}} \times (\beta^{-1} + 1). \tag{3}$$

Since the opening time and closing time of the valve do not affect the volume of individual dispersed droplets, it can be simply considered that the number of droplets is proportional to the total volume of all droplets in each droplet group. When the T_{off} remains unchanged, the number of large droplets in each droplet group (N_{large}) increases with T_{on}, while the number of small droplets remains the same ($N_{\text{small}} = 1$, $T_{\text{off}} = 0.3$ s). The total volume of the droplet group increases. According to Eq (2), the droplet quantity ratio should be proportional to the valve switching ratio, which is consistent with the fitting result as shown in Fig. 2(d). Similarly, when T_{on} keeps unchanged, N_{large} remains the same ($N_{\text{large}} = 2$, $T_{\text{on}} = 0.2$ s), but the number of small droplets N_{small} increases with T_{off}, and the total volume of the droplet group should also increase. According to Eq. (3), α^{-1} should be proportional to β^{-1}, which is also consistent with the result given in Fig. 2(e).

3.2. Effect of flow rate on droplet group

The influences of the flow rates of continuous and dispersed phases on the formation of droplet groups are also studied. Figures 3(a) and 3(d) show the formation of droplet groups under two types of conditions where the switch time of the electromagnetic valve remains unchanged, but the flow rate of the dispersed phase Q_{d} increases from 0.5 μL/min to 1.5 μL/min, and the flow rate of the continuous phase Q_{c} increases from 4 μL/min to 11 μL/min, respectively. It can be seen that the droplets still appear periodically in the form of droplet groups, and the number ratio of the large droplets (marked in red) to small droplets (marked in blue) in each droplet group remains constant under the same conditions. In addition, the change of flow rates of both the dispersed phase and the continuous phase does not affect the number of small droplets in the droplet group, but only changes the number of large droplets. Specifically, when the flow rate of the dispersed and continuous phases increases, the number of small droplets in each drop group remains at 1, but the number of large droplets gradually increases from 1 to 6, as shown in Fig. 3(c). The two-phase flow rate ratio is denoted by γ, where $\gamma = Q_{\text{d}}/Q_{\text{c}}$. Figure 3(d) shows the relationship between α and γ when Q_{d} is varied. Figure 3(e) shows the relationship between α and γ^{-1} when Q_{c} is varied. The linear relationship between α and γ is $\alpha = 15.0085\gamma - 1.503$, the linear relationship between α and γ^{-1} is $\alpha = 0.325\gamma^{-1} - 1.859$, and the linear correlation coefficients R^2 of the fitted lines are 0.9999, 0.93716, respectively, which means that the fit is very good, and there is a strong correlation between the flow rate and the droplet quantity. The linear relationship is consistent with Ward's conclusions.[25]

Then, we analyze the linear relationship between the droplet quantity ratio α ($\alpha = N_{\text{large}}/N_{\text{small}}$) and the flow rate ratio γ ($\gamma = Q_{\text{d}}/Q_{\text{c}}$) given in Figs. 3(d) and 3(e).

We rewrite Eq. (1) as

$$V_{\text{G}} = Q_{\text{c}} \times \gamma \times (T_{\text{on}} + T_{\text{off}}). \tag{4}$$

When the continuous phase flow rate Q_{c} and the valve opening and closing time ($T_{\text{on}} + T_{\text{off}}$) are constant, the size of a single droplet is almost unaffected and the number of small droplets remains unchanged ($N_{\text{small}} = 1$) all the time. As the flow rate of the dispersed phase increases, the increase in the total volume of the droplet group should be manifested as an increase in the number of large droplets. Therefore, the droplet quantity ratio should be proportional to the flow rate ratio according to Eq. (4), which is in line with the fitting relationship given in Fig. 3(d).

When the flow rate of the dispersed phase and the switching period remain unchanged, according to Eq. (1), the sum of the volumes of all droplets in the droplet group should remain constant. However, as the flow rate of the continuous phase (Q_{c}) increases, the squeezing of the dispersed phase liquid intensifies, resulting in a reduction in the volume of the generated individual droplets. Therefore, the number of droplets increases (mainly the number of large droplets), which leads to a linear relationship between the droplet quantity ratio and the flow rate ratio as shown in Fig. 3(e).

Figure 3(f) shows the volumes of a single large droplet (hollow circle), a single small droplet (solid circle), and all droplets in the group (solid triangle) at a varied flow rate of the dispersed phase. Still using the product of the area of the droplet image and the height of the chip to calculate the volume of the droplet group, the error bars in Figs. 3(f)–3(g) are obtained by calculating the standard deviation of the volume data of the four droplet groups. It suggests that there is no significant change in the volume of each large or small droplet in the droplet group, but the total volume of all the droplets in one droplet group increases with the increase of Q_{d}. The reason is that in one opening and closing cycle of the valve, the greater the flow rate of the dispersed phase, the more fluid used to generate droplets, and the sum of the volumes of all droplets in the droplet group would of course be larger. The experimental measured values are in good agreement with the theoretical predicted values calculated by Eq. (1). However, as demonstrated in Fig. 3(g), with the increase of continuous

phase flow rate, the volume of the single large droplet (hollow circle) and single small droplet (solid circle) in each droplet group gradually decreases, because the larger the continuous phase flow, the more strongly it squeezes the dispersed phase, and the smaller the droplet is generated, which accords with the general law of microfluidic droplet. Moreover, when the flow rate of the dispersed phase and the opening and closing time of the valve are unchanged, the volume sum of all droplets in the droplet group should be a fixed value according to Eq. (1), but the experimental measurement results are less than the predicted value (0.0025 μL). The possible reason is that when the continuous phase flow rate is large enough, it squeezes the dispersed phase too intensely. Then the actual flow rate of the dispersed phase is smaller than its set value, resulting in numerical inconsistency. Because the tetrafluoroethylene capillary used in the experiment has good elasticity, it is capable of accumulating some dispersed phase fluid in the pipeline. As shown in Fig. 3(b), the size of the droplets in the droplet group is indeed affected by the continuous phase flow rate. Taking the large droplet as an example, we have plotted its diameter versus the continuous phase flow rate in Fig. 3(h). According to the work of John Collins (Collins *et al.*, 2007 Microfluid Nanofluid),[26] the droplet radius (R) and the flow rate (Q) follow a quantitative relationship

$$R = \sqrt[3]{\frac{3Q_{\mathrm{d}}T_{\mathrm{g}}}{4\pi}}, \tag{5}$$

where T_{g} is the droplet generation period and T_{g} is calculated as follows:

$$T_{\mathrm{g}} = \frac{\pi^4}{3}\left(\frac{C_{\mathrm{S}}\sigma}{C_{\mathrm{D}}\rho_{\mathrm{c}}}\right)^{3/2}\frac{D_{\mathrm{c}}^6 D_{\mathrm{d}}^{3/2}}{Q_{\mathrm{d}}Q_{\mathrm{c}}^4}. \tag{6}$$

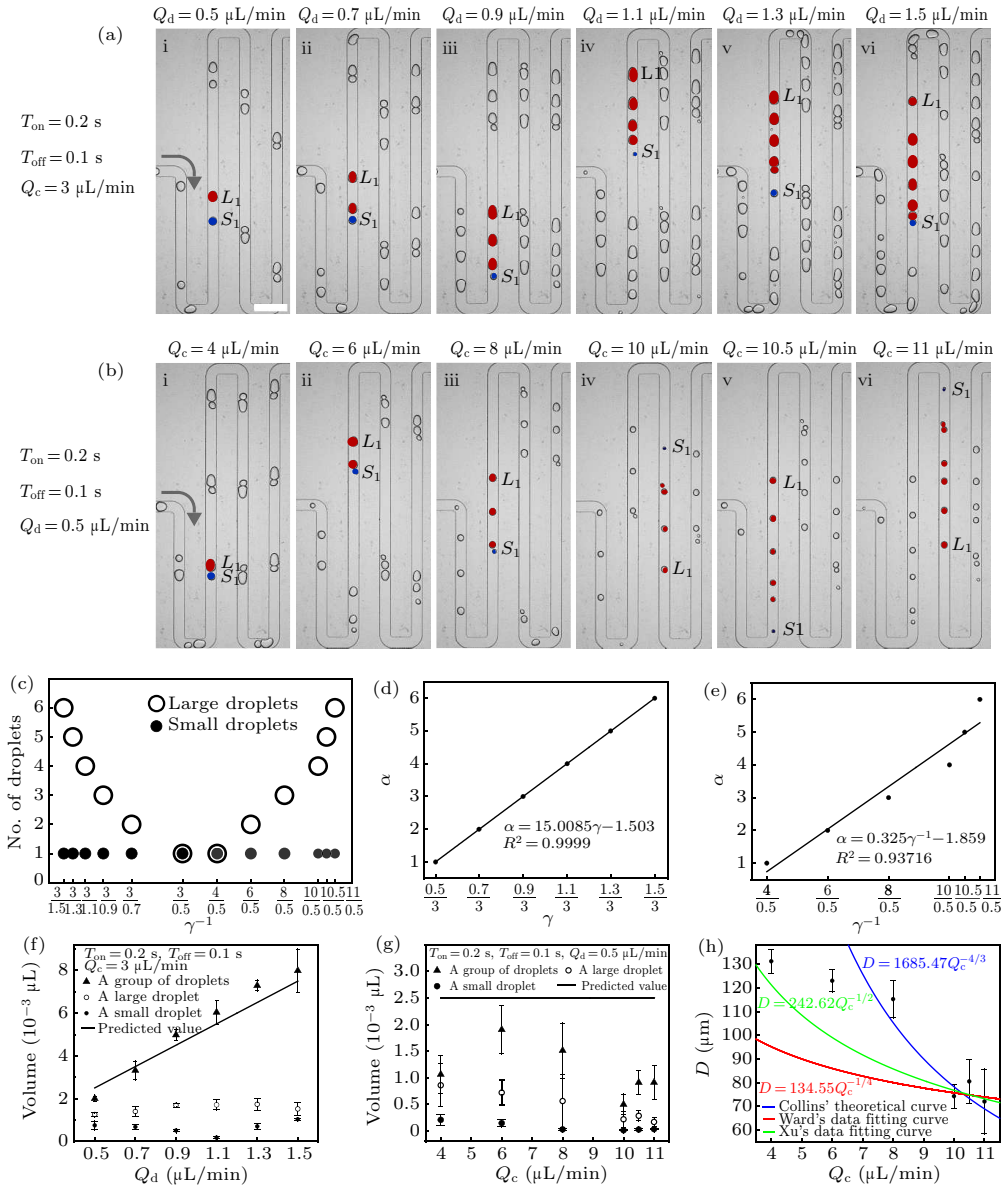


Fig. 3. (a) Representative pictures of six droplet groups with different flow rates of dispersed phase Q_{d}. The scale bar is 500 μm. (b) Representative pictures of six droplet groups with different flow rates of continuous phase Q_{c}. (c) Plot of the number of droplets versus γ^{-1}. (d) Plot of droplet number ratio γ ($\gamma = Q_{\mathrm{d}}/Q_{\mathrm{c}}$). (e) Plot of droplet number ratio α versus flow rate ratio γ^{-1}. (f) and (g) Plots of droplet volume versus Q_{d} and Q_{c}. (h) Plot of continuous phase flow rate Q_{c} versus diameter of the large droplet in each droplet group.

Combining Eqs. (5) and (6), the relationship between radius (R) and flow rate (Q) is obtained

$$R = \frac{\pi}{\sqrt[3]{4}} \left(\frac{C_S \sigma}{C_D \rho_c} \right)^{1/2} D_c^2 D_d^{1/2} Q_c^{-4/3}, \tag{7}$$

where C_S and C_D are the drag coefficient and the coefficient of interfacial tension, respectively, ρ_c is the density of the continuous phase, σ is the interfacial tension, Q_c, Q_d and D_c, D_d are the flow rate and diameter of the continuous and dispersed phase channels, respectively. Equation (7) suggests that the diameter of the droplet should be proportional to the $-4/3$ power of the continuous phase flow rate. In addition to Collins' theory, we have also found two more quantitative relationships between the droplet size and the flow rate of continuous phase (Q_c), proposed by Ward and Xu, respectively. According to the work of Thomas Ward (Ward *et al.*, 2005 Electrophoresis),[25] there is a relationship between droplet diameter (D) and flow rate (Q)

$$\frac{D}{a} \propto \left(\frac{Q_d}{Q_c} \right)^{1/4}, \tag{8}$$

where a is the microchannel width. Equation (8) states that the droplet diameter should be proportional to the $-1/4$ power of the continuous phase flow rate. According to the work of Xu (Xu *et al.*, 2006 *Lab Chip*),[27] there is a relationship between droplet diameter (D) and flow rate (Q)

$$\frac{D}{a} \propto \left(\frac{Q_d}{Q_c} \right)^{1/2}, \tag{9}$$

where a is the microchannel width. Equation (9) states that the droplet diameter (D) should be proportional to the $-1/2$ power of the continuous phase flow rate (Q_c). We have plotted all three theoretical curves in Fig. 3(h). Comparatively speaking, Collins' theory is more in line with our experimental result than the other two theories.

3.3. Pulse flow explains the droplet group phenomenon

Finally, we try to explain the seemingly counter-intuitive phenomenon that the longer the valve is open, the larger the number of droplets; the longer the valve is closed, the smaller droplets there are. We surmise that this is most likely caused by the sudden change in flow rate due to unwanted pressure pulses induced by the opening and closing of the valve. Figure 4(a) shows a group of droplet generation observed during one opening and closing cycle of the valve at experimental parameters of $T_{on} = 0.4$ s, $T_{off} = 0.3$ s, $Q_c = 3$ μL/min, and $Q_d = 0.5$ μL/min, which consists of three large droplets and one small droplet. We take the moment when the last droplet of the previous group of droplets is just generated as the zero moments, and we can see that the three large droplets in the group are generated at 0.153 s, 0.299 s, and 0.44 s respectively, which is close to the opening time of the valve of 0.4 s. The moment when the small droplets are just generated is 0.72 s, which is close to the opening and closing cycle of the valve, and also opens the generation of the next group of droplets. At the same time, the time interval between the appearance of this small droplet and the generation of the third large droplet just above it is 0.28 s, close to the valve closing time of 0.3 s. Therefore, it is reasonable to surmise that large droplets are generated during the opening phase of each opening and closing cycle of the valve, while small droplets are generated during the closing phase. This is consistent with the earlier observation that T_{on} affects the number of large droplets in the droplet group and T_{off} determines the number of small droplets in the droplet group experimentally but is still counterintuitive. Therefore, we measured the flow rate of the continuous phase in real time using a flow meter (Flow Unit, Fluigent, France). Figure 4(b) shows the continuous phase flow measured using a flow meter for one cycle under the same conditions as in Fig. 4(a). Where the valve opens at t_1, the valve closes at t_2, and the valve opens at the next cycle of t_3, $\Delta t_1 = 0.402$ s indicates the period from t_1 to t_2, and $\Delta t_2 = 0.297$ s indicates the period from t_2 to t_3. Based on the numerical magnitude relationship, it is easy to derive that Δt_1 stands for T_{on}, and Δt_2 stands for T_{off}. Contrary to expectations, the flow rate of the continuous phase drops sharply when the valve opens at t_1 and starts to rise sharply when the valve closes at t_2. To further validate this result, additional tests were performed. Figure 4(c) shows the change in the flow rate of the fluid in the pipeline over some time from when the valve is suddenly opened to when it has been kept open. It can be seen that the flow rate in the pipeline is zero before the valve is opened, but the moment the valve is first opened, there is a sudden pulse of negative and high flow rate of fluid flow through the pipeline before it returns to zero flow rate. This means that when the valve is first opened, the valve will first push the liquid flow in the reverse direction. It is not until after a longer period (about 120 s) that a positive and gradually increasing fluid flow begins to occur in the pipe. Figure 4(d) shows the influence of valve closure on the continuous phase flow rate. In the first 20 seconds, we keep the valve open all the time and set the flow rate of the continuous phase at 3 μL/min. The measured actual flow rate is stably maintained at 2.64 μL/min, which is close to the set value. Then the valve is suddenly closed and maintained. It can be seen that the flow rate does not decrease immediately. Instead, it rises rapidly to 30.59 μL/min. That is to say, the sudden closing of the valve exerts a very strong positive driving force on the fluid. The continuous phase flow rate gradually decreases to zero within approximately 90 seconds thereafter. In the experiment, the valve is constantly opened and closed, and the switching time does not exceed one second. This suggests that during the time period when the valve is closed, the continuous

phase fluid does not stop flowing. Instead, it flows at a much higher rate than when the valve is open. These flow measurements provide ample evidence of the phenomenon observed in our experiments, *i.e.*, the continuous-phase flow rate is lower when the valve is open than when the valve is closed, favoring the formation of large droplets. To explain the droplet size dichotomy, we have measured the flow rate of the continuous phase fluid, which is controlled by the valve. We find that in the case of periodic opening and closing of the valve, the flow rate of the continuous phase fluid presents a periodic square wave pulse waveform. Taking $T_{\text{on}} = 0.4$ s and $T_{\text{off}} = 0.3$ s as an example, the flow rate curve of multiple cycles is shown in Fig. 4(e). During the rapid switching process of the valve, the flow rates of the continuous phase are relatively stable in both the low flow state (marked in red, corresponding to the opening of the valve) and the high flow state (marked in blue, corresponding to the close of the valve), thereby forming large-sized and small-sized uniform droplets respectively.

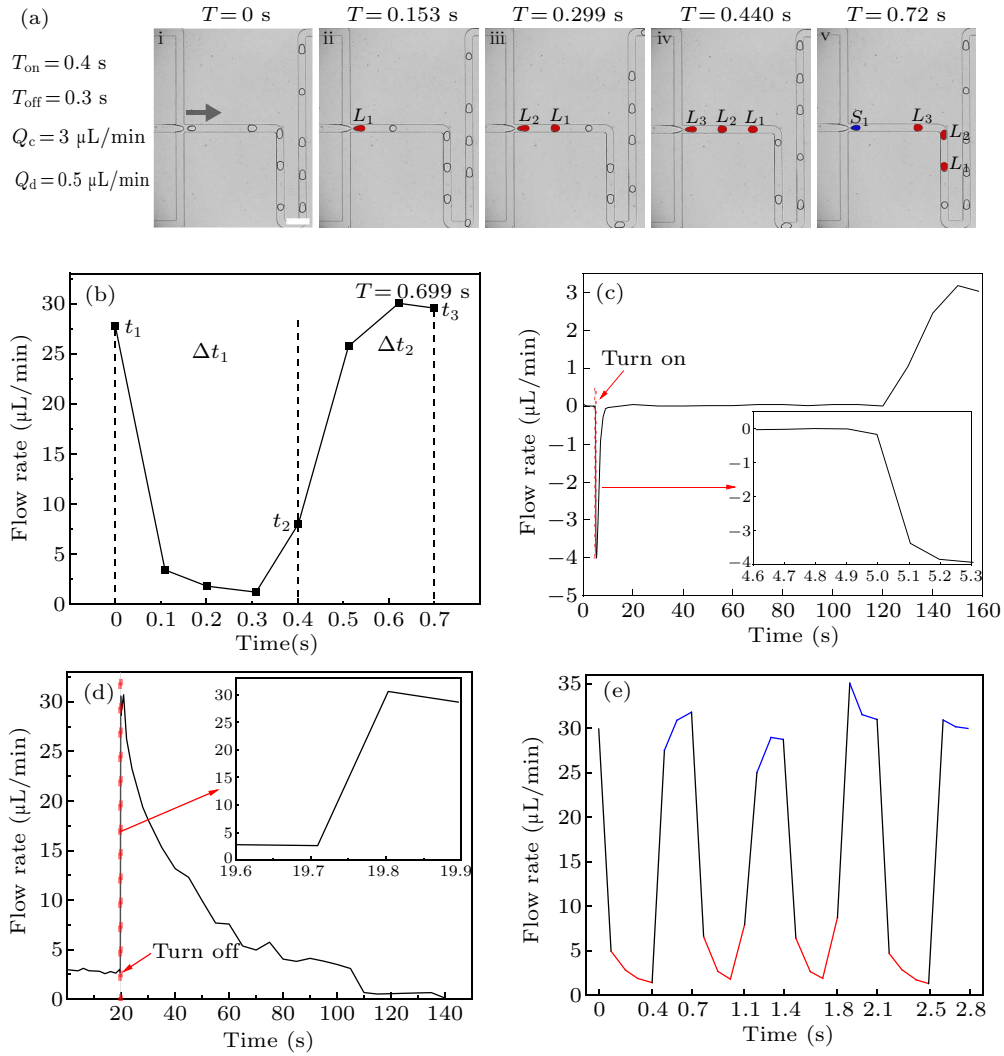


Fig. 4. (a) Snapshots of the generation of a droplet group with three large droplets and one small droplet during a switching cycle of the valve. The scale bar is 500 μm. (b) The corresponding flow rate of the continuous phase. (c) The flow rate profile in the continuous phase when the valve opens suddenly. (d) The flow rate profile in the continuous phase when the valve closes suddenly. (e) Continuous phase flow rate curve with multiple cycles at $T_{\text{on}} = 0.4$ s, $T_{\text{off}} = 0.3$ s.

4. Conclusions

In summary, we have externally connected a programmable electromagnetic valve with a traditional microfluidic chip, and by opening and closing the valve periodically, we have achieved the generation of droplet groups with the controllable number and volume of droplets in the microchannel in one switching cycle of the valve, and have revealed the underlying physics. Specifically, the valve opening time and two-phase flow rate determine the number of large droplets in the droplet group, and the valve closing time determines the number of small droplets. The volume of a single droplet depends mainly on the flow rate of the continuous phase. Our study enriches the understanding of microfluidic droplet formation. It provides an efficient approach for the preparation of polydisperse droplets, which is important for microfluidic chip-based droplet control and may find potential applications in areas related to microfluidic droplets. Generating droplet groups with variable droplet sizes is important for drug deliv-

ery, and drug screening applications such as eutectic screening. Each droplet can be used as a bioreactor, and droplets with different volumes can meet the need for differentiated drug volumes, which may facilitate the development of high-performance chemistry and bioanalysis.

Acknowledgements

Project supported by the Chongqing Human Resources and Social Security Bureau (Grant No. CX2023079), the Fundamental Research Funds for the Central Universities, China (Grant Nos. 2023CDJXY-049 and 2024CDJXY-022), and the National Natural Science Foundation of China (Grant Nos. T2350007 and 127404).

References

[1] Chiu D T and Lorenz R M 2009 *Accounts Chem. Res.* **42** 649
[2] Grossier R, Hammadi Z, Morin R and Magnaldo A 2011 *Appl. Phys. Lett.* **98** 3
[3] Chen L, Yang C, Xiao Y, Yan X, Hu L, Eggersdorfer M, Chen D, Weitz D A and Ye F 2021 *Mater. Today Nano* **16** 100136
[4] Chan H F, Zhang Y and Leong K W 2016 *Small* **12** 2720
[5] Mazutis L, Baret J C and Griffiths A D 2009 *Lab Chip* **9** 2665
[6] Mashaghi S, Abbaspourrad A, Weitz D A and van Oijen A M 2016 *Trac-Trends Anal. Chem.* **82** 118
[7] Gielen F, Hours R, Emond S, Fischlechner M, Schell U and Hollfelder F 2016 *Proc. Natl. Acad. Sci. USA* **113** E7383
[8] Seong G H, Heo J and Crooks R M 2003 *Anal. Chem.* **75** 3161
[9] Miller O J, El Harrak A, Mangeat T, Baret J C, Frenz L, El Debs B, Mayot E, Samuels M L, Rooney E K, Dieu P, *et al.* 2012 *Proc. Natl. Acad. Sci. USA* **109** 378
[10] Vladisavljevic G T, Khalid N Neves M A, Kuroiwa T, Nakajima M, Uemura K, Ichikawa S and Kobayashi I 2013 *Adv. Drug Deliv. Rev.* **65** 1626
[11] Yang Z, Chen J, Xiao Y, Yang C, Zhao C X, Chen D and Weitz D A 2024 *Chem. & Bioengineering* **1** 2
[12] Colmenares J C, Varma R S and Nair V 2017 *Chem. Soc. Rev.* **46** 6675
[13] Zhang D T, Wu F X, Peng M H, Wang X Y, Xia D G and Guo G S 2015 *J. Am. Chem. Soc.* **137** 6263
[14] Guo M T, Rotem A, Heyman J A and Weitz D A 2012 *Lab Chip* **12** 2146
[15] Huebner A, Sharma S, Srisa-Art M, Hollfelder F, Edel J B and Demello A J 2008 *Lab Chip* **8** 1244
[16] Nan L, Zhang H D, Weitz D A and Shum H C 2024 *Lab Chip* **24** 20
[17] Shang L R, Cheng Y and Zhao Y J 2017 *Chem. Rev.* **117** 7964
[18] deMello A J 2006 *Nature* **442** 394
[19] Zeng S J, Li B W, Su X O, Qin J H and Lin B C 2009 *Lab Chip* **9** 1340
[20] Guzowski J, Korczyk P M, Jakiela S and Garstecki P 2011 *Lab Chip* **11** 3593
[21] Churski K, Nowacki M, Korczyk P M and Garstecki P 2013 *Lab Chip* **13** 3689
[22] Zhang Y Y, Xia H M, Wu J W, Zhang J and Wang Z P 2019 *Appl. Phys. Lett.* **114** 073701
[23] Yao J R, Li G Q, Yao X Y, Zhou L J, Ye Z K, Liu Y P, Zheng D T, Tang T, Song K N, Chen G and Liu L L 2024 *Chin. Phys. B* **33** 058706
[24] Cybulski O, Jakiela S and Garstecki P 2016 *Lab Chip* **16** 2198
[25] Ward T, Faivre M, Abkarian M and Stone H A 2005 *Electrophoresis* **26** 3716
[26] Collins J and Lee A P 2007 *Microfluidics and Nanofluidics* **3** 19
[27] Xu J H, Luo G S, Li S W and Chen G G 2006 *Lab Chip* **6** 131